A THEORETICAL AND EXPERIMENTAL STUDY OF

REJECTION SURGES IN TRAPEZOIDAL CHANNELS

by

Danny Lee King

B.S.C.E., University of Idaho, 1960

A thesis submitted to the Faculty of the Graduate

School of the University of Colorado in partial

fulfillment of the requirements for the Degree

Master of Science

Department of Civil Engineering

1966

This thesis for the Master of Science degree by

Danny Lee King

has been approved for the

Department of

Civil Engineering

by

W. W. Dehoff

J. Ernest Flack

Date *March 28, 1966*

King, Danny Lee (M.S., Civil Engineering)

A Theoretical and Experimental Study of Rejection Surges in
    Trapezoidal Channels

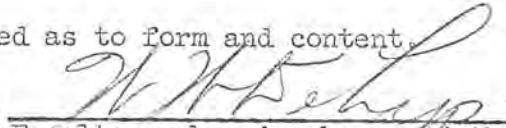Thesis directed by Professor Warren De Lapp

Theoretical equations and supporting experimental data are presented for the determination of the size, velocity, and shape of surge waves in a trapezoidal channel following complete rejection of the flow. Comparisons are made between exact and approximate theoretically derived equations and the agreement of these equations with experimental data is determined. The approximate form is found to be essentially equal to the exact form. Generally, agreement between theory and experimental data is quite good. The greatest deviation between theory and experiment occurred in the determination of the peak surge height.

Results of previous experiments on rectangular channels are summarized and reasons for disagreement among experimenters are briefly explored.

A short digital computer program was developed for the trial solution of the governing equations. An explanation of the program, the source statement listing, and sample input data and results are presented.

This abstract is approved as to form and content.

Signed
                      Faculty member in charge of thesis

ACKNOWLEDGMENTS

CONTENTS

Computer program source statements, sample input data
  sheet, and sample output listing

LIST OF TABLES

LIST OF FIGURES

NOMENCLATURE

Symbol	Units	Description
A_1	Ft^2	Flow area preceding surge
A_2	Ft^2	Flow area following surge
B	Ft	Bottom width of channel
c	Ft/sec	Celerity of wave
D_1	Ft	Hydraulic depth preceding surge
F	Lbs	Force, in momentum equation
Fo	Dimensionless	Froude Number of flow preceding surge
Fw	Dimensionless	Froude Number of surge wave
g	Ft/sec^2	Acceleration of gravity
h	Ft	Average surge height
$\bar{h}$	Ft	Distance from the center of gravity of the surge area to the top surface of the surge
H	Ft	Depth of flow preceding surge (also y_1)
h_{max}	Ft	Maximum surge height
L	Ft	Wave length
p	Lbs/ft^2	Pressure, in momentum equation
Q	Ft^3/sec	Discharge
S	Dimensionless	Channel side slopes
T	Ft	Channel top width
V_1	Ft/sec	Velocity of flow preceding surge
V_2	Ft/sec	Velocity of flow following surge
Vw	Ft/sec	Surge wave velocity
x	Ft	Horizontal distance from origin

Symbol	Units	Description
y_1	Ft	Depth of flow preceding surge (also H)
$\bar{y}_1$	Ft	Centroid of flow depth preceding surge, measured from surface
$\bar{y}_2$	Ft	Centroid of flow depth following surge, measured from surface
γ	Lb/ft^3	Unit weight of water
ρ	Slug/Ft^3	Mass density of water

CHAPTER I
INTRODUCTION

Water surface waves can be classified in two main categories:
capillary waves and gravity waves. Capillary waves are formed
through the effects of surface tension, the relative influence
of which is expressed by the Weber Number. The form of the cap-
illary wave is dependent upon the depth of the water body in which
the wave is formed, the wave length, and the wave height. Capil-
lary waves are generally observed as wind ripples and similar
oscillatory phenomena.

In contrast to the capillary wave, the gravity wave, as the
name implies, is formed under the influence of gravity as expressed
in the dimensionless ratio of the Froude Number. Gravity waves are
further classified as oscillatory or translatory. The oscillatory
wave is created by a periodic disturbance such as the forward and
backward movement of a bulkhead in a channel or the movement of a
paddle wheel. The translatory gravity wave is a result of sudden
permanent displacement of a body of water. A special form of the
translatory wave is the solitary wave created, for example, by the
movement of a channel bulkhead to displace a finite volume of fluid.
The shape of the solitary wave, in contrast to the capillary wave,
is dependent only on the liquid depth and the wave height. Solitary
waves include such varied phenomena as tidal waves, seismic waves
(in the earth's crust), flood waves, bore waves, and open channel
surge waves.

Open channel surges, which can be described as moving hydraulic jumps, are the subject of this thesis. In general, open channel surges may be classified according to the means of formation and the direction of propagation. That is, they may be catalogued as positive or negative, and upstream or downstream (sometimes described as ascending or descending). A positive surge forms with rejection of flow in a channel or upon a sudden release of flow into a channel and results in a rising water surface. The negative surge results from a rapid release of flow from a channel or a rapid decrease in the supply of flow into a channel, characterized by a falling water surface. Several examples of the formation of the characteristic surge types are: (1) a positive downstream surge formed by rapid opening of a sluice gate at the upstream end of a channel, (2) a negative downstream surge formed by rapid closing of a sluice gate at the upstream end of a channel, (3) a negative upstream surge formed by rapid opening of a sluice gate at the downstream end of a channel, and (4) a positive upstream surge formed by rapid closing of a sluice gate at the downstream end of a channel. All four types exemplify problems encountered in the design of channels leading to and from pumping or power plants. This thesis will be restricted to discussion of surge type (4). It should be recognized, however, that the basic equations are equally applicable to the other three types.

Positive upstream surges occur in pumping or power canals following rejection of flow from the pumps or turbines due to power failure or changes in load requirements. These surges may result in costly freeboard requirements to prevent channel bank damage. It is necessary, therefore, to obtain accurate information as to the size, shape, and velocity of propagation of the rejection surges.

Often only general approximate equations are provided for the determination of the height and velocity of open channel surges. In many cases these approximations are adequate; but, often the limits of design are such that more accurate relationships become necessary.

In this thesis the writer presents, with supporting experimental data, appropriate equations for the formation and propagation of rejection surges in trapezoidal channels. The trapezoidal shape is considered because of its relatively common use in modern irrigation practice. It should be noted, however, that a similar approach would be taken for other channel shapes. Many theoretical and experimental studies have been made for rectangular channels.

CHAPTER II
THEORETICAL CONSIDERATIONS

The form of a positive upstream rejection surge is dependent on the depth and velocity of the initial flow in the channel, the shape of the channel cross-section, friction, and the velocity distribution of the initial flow. For relatively small surge heights, where the ratio of the average surge height (h) to the initial flow depth (y_1) is less than approximately 0.28 (determined experimentally for rectangular channels), the rejection surge will be undular in form, consisting of a series of oscillation peaks superimposed upon the average surge height. Above the $\frac{h}{y_1}$ ratio of 0.28, the surge will become unstable and will eventually break and assume a form without oscillation peaks. These forms resemble those of the hydraulic jump. The undular shape is characteristic at Froude Numbers between 1.0 and approximately 1.7, and the direct shape at Froude Numbers above 1.7.

Derivation of basic equations for average surge height and velocity

The principles of continuity and momentum form the basis for the development of equations for the height and velocity of a surge. As mentioned previously, this development will be restricted to a positive, ascending (upstream) surge in a trapezoidal channel, following complete or partial rejection of the initial flow. The derivation, though not unusual or rigorous, is often restricted to rectangular channels. The end result of the writer's derivation can also be found in Chow's text [4] .1/

_____

1/Numbers in brackets refer to references listed at the end of this thesis.

A definition sketch of a positive ascending surge is shown in Figure 1. The form of the wave is idealized; the oscillation peaks are absent and the profile resembles that of a direct wave form.

Through considerations of momentum:

$$\gamma A_2 \bar{y}_2 - \gamma A_1 \bar{y}_1 = \frac{\gamma}{g}(Vw+V_2)A_2(V_1-V_2)$$

$$A_2 \bar{y}_2 - A_1 \bar{y}_1 = \frac{1}{g}(Vw+V_2)A_2(V_1-V_2) \tag{1}$$

and by continuity:

$$Q = V_1 A_1 - Vw(A_2-A_1) = V_2 A_2$$

$$V_2 = \frac{V_1 A_1 - VwA_2 + VwA_1}{A_2} \tag{2}$$

Substituting (2) into (1):

$$A_2 \bar{y}_2 - A_1 \bar{y}_1 = \frac{1}{g}\left[Vw+\frac{V_1 A_1 - Vw(A_2-A_1)}{A_2}\right]A_2\left[V_1-\frac{V_1 A_1 - VwA_2 + VwA_1}{A_2}\right]$$

$$A_2 \bar{y}_2 - A_1 \bar{y}_1 = \frac{1}{g}(V_1+Vw)^2 A_1(1-\frac{A_1}{A_2})$$

$$(V_1+Vw)^2 = \frac{g(A_2 \bar{y}_2 - A_1 \bar{y}_1)}{A_1(1-\frac{A_1}{A_2})}$$

$$Vw = \sqrt{\frac{g(A_2 \bar{y}_2 - A_1 \bar{y}_1)}{A_1(1-\frac{A_1}{A_2})}} - V_1 \tag{3}$$

Rearranging Equation (2):

$$Vw = \frac{V_1 A_1 - V_2 A_2}{(A_2 - A_1)} \tag{4}$$

Equations (3) and (4) may be solved by trial.

For easier comparison with other derivations the equations can be converted to those concerned with rectangular channels, in which $A = B\, y$, and $\bar{y} = \frac{y}{2}$:

$$Vw = \sqrt{\frac{g y_2}{2 y_1} (y_1 + y_2)} - V_1 \tag{5}$$

and

$$Vw = \frac{V_1 y_1 - V_2 y_2}{y_2 - y_1} \tag{6}$$

The celerity of the wave, c, is equal to the wave velocity, Vw, plus the initial flow velocity, V_1.

Denoting the surge height, $y_2 - y_1$, by h:

$$c = \sqrt{\frac{g y_2}{2 y_1} (y_1 + y_2)} = \sqrt{\frac{g(h + y_1)}{2 y_1} (h + 2 y_1)}$$

$$= \sqrt{\frac{g(h^2 + 3 y_1 h + 2 y_1^2)}{2 y_1}}$$

$$= \sqrt{g\left(\frac{h^2}{2 y_1} + \frac{3}{2} h + y_1\right)} \tag{7}$$

which was originally presented by Saint-Venant [12].

Other hydraulicians have derived similar relations using different approaches. Keulegan and Patterson [9], in 1940, began their derivation with Boussinesq's formula [2]:

$$c = \sqrt{gy_1}\left(1 + \frac{3}{4}\frac{h}{y_1} + \frac{y_1^2}{6h}\frac{\partial^2 h_{max}}{\partial x^2}\right) \tag{8}$$

where h_{max} is the peak height of the oscillations, Figure 2, and x is the horizontal distance in the direction of motion. The term $\frac{\partial^2 h_{max}}{\partial x^2}$ represented the curved front of the surge. The oscillation peak will be discussed in detail later. At the inflection points of the oscillations the surge height is equal to the final surge height and the partial derivative term vanishes, leaving the equation

$$c = \sqrt{gy_1}\left(1 + \frac{3}{4}\frac{h}{y_1}\right) \tag{9}$$

Squaring the parenthetical term results in

$$c = \sqrt{gy_1\left[1 + \frac{3}{2}\frac{h}{y_1} + \frac{9}{16}\left(\frac{h}{y_1}\right)^2\right]}$$

or

$$c = \sqrt{g\left(\frac{9}{16}\frac{h^2}{y_1} + \frac{3}{2}h + y_1\right)} \tag{10}$$

which is essentially identical to Equation (7) above except that $\frac{1}{2}\frac{h^2}{y_1}$ is replaced by $\frac{9}{16}\frac{h^2}{y_1}$.

Returning now to Equation (3) for trapezoidal channels, the wave celerity is expressed by

$$c = \sqrt{\frac{g(A_2\bar{y}_2 - A_1\bar{y}_1)}{A_1\left(1 - \frac{A_1}{A_2}\right)}} \tag{11}$$

Favre [5], through continuity and momentum considerations, derived

$$c = \sqrt{g\left(A_1 \frac{h}{A_2 - A_1} \div \bar{h}\right)\left(1 \div \frac{A_2 - A_1}{A_1}\right)} \qquad \text{(11a.)}$$

where $\bar{h}$ is the distance from the center of gravity of the surge area $(A_2 - A_1)$ to the top surface of the surge. Favre's notation has been changed to that used in this thesis. This equation is identical to Equation (11). Favre developed an approximate form by (1) assuming that $\bar{h} = \frac{h}{2}$, (2) putting $(A_2 - A_1)$ in terms of h, and (3) multiplying the parenthetical terms and neglecting all h^2 terms. The approximate form of Equation (11a.) is

$$c = \sqrt{gD_1}\left[1 \div \left(1 - \frac{2S}{3}\frac{D_1}{T}\right)\frac{3}{4}\frac{h}{D_1}\right] \qquad \text{(12)}$$

in which S is the channel side slope, T the water surface top width, and D_1 the hydraulic depth. To compare Equation (12) with the others for rectangular channels, set $S = 0$. It is found that Equation (12) will now be identical to Equation (9) of Keulegan and Patterson. Equations (11) and (12) will be compared to determine the error, if any, in using Favre's approximate relationship for the surge celerity.

Derivation of relationship for maximum height of oscillation peaks

Using the method proposed by Jones [8], a relation for the height of the maximum undular peak can be formed. Equations (11) and (12) express the celerity of a wave of direct form (without oscillation peaks) in a trapezoidal channel. By making a basic

assumption that the undular wave consists of a series of solitary waves superimposed upon a wave of direct form, the celerity of the direct form is equated to that of a solitary wave and a relationship is found for the peak height.

The equation for the celerity of a solitary wave is $c = \sqrt{gD}$, where D is the hydraulic depth. $D = \dfrac{A}{T}$, where A is the area and T the water surface top width of a trapezoidal channel. If c is also the celerity of the direct wave, then

$$\sqrt{gD} = c$$
$$gD = c^2$$
$$D = \frac{c^2}{g} \tag{13}$$

The height of the maximum oscillation peak can be derived from this expression.

Calculations by digital computer

Equations (4) and either (11) or (12) involve trial solutions for the two unknown variables, V_2 and y_2. To facilitate rapid solutions of these equations for a large number of conditions, a computer program was developed for use on the Honeywell H-800 computing facility, Bureau of Reclamation, Denver, Colorado. The program is written in the AUTOMATH (FORTRAN IV) programing language. The original form of the program included the solution of Equations (4), (11), and (13). The program was then revised to substitute

Equation (12) for Equation (11) and the results were compared.
A listing of the program and samples of the input and output data
are included in the Appendix.

Input data consists of the conveyance channel geometry, the
initial rate of flow (Q), the rejected rate of flow (QREJ), and the
size (DELTA) and number (N) of iteration steps used in the solution
of the equations. The channel geometry is described by the initial
flow depth (Y1), the bottom width (B), and the side slopes (S).
Output includes the input factors plus the Froude Number of the
initial flow (F or Fo), the ratio of average surge depth to initial
depth (YAVE), the ratio of peak surge depth to initial depth (YPK),
the ratio of peak surge depth to average surge depth (RATIO), the
wave velocity (W), the wave celerity (C), the initial flow velocity
(V1), and an indicator of the accuracy of the approximate solution (FF).

The bisection method is used to derive an approximate solution
for the average surge depth. When V_1 is added to Equations (11) or
(12) they are identical to Equation (4), since each then represents
the wave velocity. Their difference, represented by the symbol FF
in the program, is zero when the correct value for y_2 is substituted.
Beginning with an assumed value for y_2, outside the expected range of
the correct solution, successive approximations are made until the
value of FF is within an arbitrarily small range of values close to
zero. The iteration is halted when the value of FF is smaller than
the selected value (0.00001 fps in this case) or when the specified

number of iterations has been performed. The final value of FF is printed as a check.

After the values of the average surge depth (and thus the wave celerity) have been determined, Equation (13) is used to determine the depth corresponding to the height of the maximum oscillation peak. The results are tabulated in Table 1 and are presented graphically in Figures 3, 4, and 5.

Discussion of results of theoretical analysis

Table 1 shows that the average surge heights and velocities determined from either Equation (11) or Equation (12) are essentially identical. Variation of the average surge height and surge velocity with the Froude Number of the initial flow is shown in Figures 3 and 4, respectively.

Computation of the peak surge height showed some variation between the two methods of computation. Because the peak height is based on the square of the surge celerity, the slight differences in wave velocity noted in Table 1 are compounded. The peak height values based on either Equation (11) or (12) were more than twice the average surge height and were considered unreasonable, according to the experiences of other investigators. This premise was supported by the present tests, as explained later in this thesis. The theoretical relationships between the average surge height and the peak surge height corresponding to the celerities computed with Equation (12) are presented in Figure 5 in dimensionless form, primarily to demonstrate the theoretical variation of the peak height with the initial depth of flow.

CHAPTER III
EXPERIMENTAL STUDIES

Review of previous investigations

Previous work in developing the theory of open channel waves
has been reviewed earlier. Experimental work in this field began,
to the best of the writer's knowledge, with that of J. Scott
Russell [15] in England in 1844, followed shortly thereafter with
experiments by H. Bazin [3], Lord Rayleigh [13], G. G. Stokes [16],
and many other well-known hydraulicians. Work in this century has
been highlighted by that of Henry Favre, whose famous paper was pub-
lished in 1935, as cited earlier in this thesis. Other fairly recent
notable accomplishments were made by G. H. Keulegan and G. W.
Patterson [9], A. T. Ippen and D.R.F. Harleman [7], J. A. Sandover
and O. C. Zienkiewicz [14], and B. Gentilini [6]. All of these
experiments, including those of Favre, were concerned with rectangular
channels. Favre's paper included some theory with reference to
trapezoidal channels as noted in Chapter II and, very recently,
C. Thirriot and S. Bednarczyk [17], mentioned that they had carried
out a theoretical investigation of trapezoidal flumes but did not
include the results in their paper. To the writer's knowledge, no
experimental data have been published on waves in trapezoidal
channels to this time (1966).

Disagreements exist among experimental observations on rec-
tangular channels for the limits of stability of the undular form
and for the surge height at which breaking occurs. Keulegan and

Patterson recorded data which indicate a stable form below $\frac{h}{y_1} = 0.275$, an unstable region between 0.275 and approximately 0.530, and breaking waves above $\frac{h}{y_1} = 0.530$. Both Gentilini and Favre recorded breaking waves above $\frac{h_{max}}{y_1} = 0.60$, where h_{max} is the height of the maximum oscillation peak. (Keulegan and Patterson's value of $\frac{h}{y_1} = 0.530$, corresponded to an $\frac{h_{max}}{y_1}$ value of about 0.58.) In 1932 Bakhmeteff [1] observed breaking above $\frac{h_{max}}{y_1} = 1.0$; Ippen and Harleman agreed with this finding in 1954 experiments. Very early experiments (1894) by McCowan [11] proposed a limit of 0.78. Keulegan and Patterson proposed a theoretical value of 0.735 but measured a value of 0.58, as stated above.

The apparent discrepancies among experimental data are due to: (1) variation in the velocity distribution of the initial flow, (2) errors inherent in the methods of measuring the wave heights, and (3) the distance from the origin of the surge to the measuring section. Keulegan and Patterson have discussed the effect of nonuniform velocity distribution on wave propagation. They found this effect to be important only in cases where the initial flow before initiation of the surge was near or above supercritical velocity. The effect becomes less important as the velocity decreases in the subcritical range. Favre also discussed this point.

Errors in the various methods of measuring wave heights include parallax in photography and other optical methods and meniscus effects and electrical instability in electronic instrumentation. The location of the measuring section is important because of the tendency for a surge wave to "build" toward a maximum height for some time after initiation.

Description of the experimental apparatus

The laboratory model used in these studies consisted of a straight trapezoidal section with a length of 48-1/2 feet, a bottom width of 1 foot, a depth of 1 foot and 1-1/2:1 side slopes, Figure 6. The channel floor was level and the floor and sides had an enamel paint finish. Water was supplied to the model through a recirculating system by a centrifugal pump. Discharges were measured with a portable orifice meter with interchangeable orifices, each of which was calibrated volumetrically. The control at the downstream end of the model consisted of a rectangular sluice gate which was used to control the depth of flow for each test discharge. The gate could be closed very rapidly by hand for almost instantaneous complete rejection of the inflow.

The model instrumentation included six capacitance type wave probes with sensors consisting of plasticized-enamel-coated wire. Each wire was about 6-1/4 inches long, mounted in a U-shaped frame made from 1/4-inch diameter stainless steel rod. The wires were held in the frames by small plastic insulators. The lower end of

the wire was carefully sealed in the insulator to prevent electrical shorting by the water. Each frame was attached to a modified point gage staff in a rack and pinion device with a vernier reading to 0.001 foot. Each probe was connected to one channel of a six-channel direct-writing oscillograph (a Sanborn recorder in this case). The locations of the probes are shown on Figure 6. Figure 7 is a photograph of the test channel and a set of probes.

The wave height is indicated by the change in capacitance as the immersion of the sensor wire is changed. The plasticized enamel coating acts as the dielectric of the capacitor whose legs consist of the wire and the water. The unsealed end of the sensor wire is connected to one leg of a resistance-capacitance bridge, Figure 8. As the water level varies on the sensor, the capacitance across the fixed capacitor C_2 also varies, resulting in imbalance of the bridge and an accompanying signal to the recorder.

Some difficulty was encountered during calibration of the wave probes. Accurate data were assured by making a separate calibration for each test run, except in one or two cases when two runs at the same depth were made in quick succession. Calibration was accomplished by raising and lowering the probes known distances in a stable pool of water formed by ponding the model channel. Wetting and drying of the coating on the wire caused non-linearity and a careful calibration routine was necessary. After establishment of the zero datum, each wire was lowered a known distance in

the pool. By lowering the probe beyond the required range, waiting for several seconds, then raising the probe to the correct position, the slow wetting process was accelerated and a stable condition was reached in 15 to 30 minutes. The probe was then raised in increments to the zero position to check the linearity.

It was necessary to carefully insulate the bridge circuit to eliminate zero datum drift caused by variation in room temperature. Also, some instability was caused by fine particles in the recirculated water which were deposited on the wire sensors.

Other experimenters [13], by comparing wave probe records with photographic records, have estimated that meniscus (surface tension) effects can result in an error of approximately plus or minus 0.015 inch (or about 0.001 foot), with the largest errors occurring at wave troughs (-0.01 to +0.02 inch). No attempt was

to evaluate the surface tension effect in the present studies; however, the cited reference indicates that errors due to this effect are not appreciable.

Test program and limitations

Test runs were planned so that a range of Froude Numbers

$(Fo = \dfrac{V_1}{\sqrt{gD_1}})$ between approximately 0.05 and 0.30 (corresponding

to the theoretical computations) could be investigated for three average flow depths in the canal: 4 inches, 6 inches, and 8 inches.

The model outlet flume was found to have insufficient capacity for a Froude Number of 0.298 at an initial depth of 6 inches, and for Froude Numbers of 0.245 and 0.306 at an initial depth of 8 inches. Therefore, those three runs were excluded. Average surge height, maximum peak height, wave velocity, wave length, and the general characteristic shape of the wave profile were determined for each test. It was attempted to limit the studies to the stable range so that no breaking of the surge front would occur. The experimental data are shown in Table 2.

Discussion of experimental results

The recorded surge wave was of the undular form, consisting of the initial wave followed by a series of secondary oscillations. In this study, the leading peak was usually the largest of the series, with reference to the initial flow depth before surge propagation. Figures 9 and 10 show a typical wave form.

The average surge height varied with the Froude Number of the initial flow as shown in Figures 11, 12, and 13. The theoretical curves of Figure 3 are included for comparison.

Figure 11 compares the experimental data with theory for an initial flow depth of 4 inches (0.333 foot). It should be mentioned at this point that the slope of the water surface was assumed to be negligible with the same depth occurring at all three probe sections. Figure 11 indicates fairly close agreement

between experiment and theory. Data   all th robes are quite
closely group. :cept at a Froude ber of 0.2 which shows
appreciable   er. This scatter   probably di o instability
of the su   It was explained   er that instability was noted
in rectang   channels for value $\frac{h}{y_1}$ above abo 0.28. It
seems reaso   that the trapez   shape coul use instability
at a lower $\bar{y}_1$ value, approximately 0.20 in this case.

The experimental data for an initial flow depth of 6 inches
(0.500 foot), Figure 12, shows that the experimental data begin
to deviate from theory at a Froude Number of about 0.10. The
deviation increases as the Froude Number increases. Similar results
were obtained for an initial flow depth of 8 inches (0.667 foot),
Figure 13. A possible explanation for the increasing deviation
is that as the surge height increases the form gradually changes
from undular to direct. This premise is supported by the apparent
instability of the surge front noted in Figure 11.

Figure 14 attempts to compare the experimental results for
the relationships among Froude Number, average surge height, and
height of the first oscillation peak. The widely scattered data
do not provide a meaningful illustration. Also, the experimental
peak heights are considerably lower than the theoretical heights
listed in Table 1. Data for Probe 3 were given special attention
because it was felt that the surge had probably attained a rela-
tively stable form upon reaching that section. These data also

failed to indicate any well defined relationship between the ratio
of $\dfrac{h_{max}}{h}$ and the Froude Number. It was decided to abandon the
attempt to find a relationship between dimensionless ratios and
to simply plot h_{max} versus h. This plot, Figure 15, indicates
that the height of the first oscillation peak is essentially a
constant multiple of the average surge height and is invariant
with respect to the initial flow depth or Froude Number. Again
the data are scattered, but an upper limit of $h_{max} = 1.253h$ is
indicated. The relationship at Probe 3 is fairly well defined
as $h_{max} = 1.13h$. A few points lie below the theoretical
lower limit, $h_{max} = h$, corresponding to a surge of direct form,
thus indicating that the first peak is not always the maximum
and can be smaller than the average surge height.

Figure 16 shows the experimental relationship between the
Froude Number of the initial flow and the wave Froude Number.
The theoretical curves of Figure 8 are included for comparison.
Figure 16 shows that the experimental wave velocities are, in
general, somewhat greater than those predicted by Equation (11)
or (12). Also, the variation of wave velocity with the initial
flow depth is not well defined and the data are somewhat scattered.
The scatter is very likely due to errors in determining, from the
oscillograph records, the time of passage of the surge between measuring
stations. The arrival of the surge at a measuring station was
indicated by the initial upward deflection of the oscillograph

trace. For some of the small surges, the stylus movement was gradual and determination of the initial deflection was very difficult.

Figure 17 illustrates the variation of the distance between the first two oscillation peaks, L, with the wave velocity. Data for only the centerline probes were plotted and no attempt was made to develop dimensionless ratios or make comparisons with theory. To the writer's knowledge, the use of such information is limited. One recent application was the determination of required delay of response in float operated automatic pump controls. The pumps were required to start or stop in response to slow variations in the intake canal water surface in order to maintain a constant water surface elevation. The velocity and wave length of the rejection surges were required so that the remaining operating pumps would not switch off and on during passage of the surge. Figure 17 shows that the length of the first wave increases as the surge moves upstream. The change in wave length from Probe 3 to Probe 5 is relatively small, which indicates that the surge is approaching a stable form.

Although a prototype surge would be attenuated by friction, the relatively short test channel did not allow evaluation of this effect. Also, Figure 17 indicates that the surge had probably not quite reached a stable form in the available distance. In fact, inspection of Table 2 shows that the maximum peak increased, in many cases, between the first two probe sections, then decreased to the third section. This deterioration is more likely caused by instability rather than friction.

J. A. Sandover and O. C. Zienkiewicz [4] contend that friction has little attenuating effect on the initial peak, but affects the trough heights and wave lengths. They present equations which describe the profile of the undular surge and the attenuation of the oscillation peaks. Following complete dissipation of the oscillation peaks, the stable wave is damped as described by Keulegan [10].

CHAPTER IV
CONCLUSIONS AND RECOMMENDATIONS

Use of either Equation (11), Equation (11a.), or Equation (12) with Equation (4) will give a satisfactory prediction for the average surge height for complete rejection of flow. Equation (12) is simplest in form and is recommended for use in hand calculations.

The error in using Equation (13) for determination of the maximum oscillation peak increases as the average surge height increases. The tests indicated that the maximum peak height is approximately 1.2 times the average surge height, as compared to the theoretical ratio of 2.1 to 2.7. The experimental data were generally independent of the initial flow depth, contrary to the indications of theory.

The experimental wave velocities showed good agreement with those predicted by theory; however, the variation with initial depth was not well defined. The experimental variation of the length of the first wave with wave velocity was determined. No theoretical predictions were made for comparison.

It is recommended that: [1] Equations (4) and (12) should be used to determine average surge height; [2] the relationship $h_{max} = 1.2h$ should be used to determine the maximum oscillation peak height; [3] Equation (12) may be used to determine the wave velocity with the knowledge that the experimental data deviated

slightly from theory; and [4] Figure 21 may be used to estimate the length of the first wave for a given wave velocity by applying the appropriate model scales based on the Froude law.

If accuracy limits greater than those presented in this study are required, there may be justification for a model study of the particular prototype configuration being investigated.

REFERENCES

1. Bakhmeteff, B. A., "Hydraulics of Open Channels." Engineering Societies Monograph, McGraw-Hill, 1932.

2. Boussinesq, J. V., "On the Steady Varied Flow of Water in Conduits and Open Channels." Comptes Rendus des Seances de l'Academie des Sciences, Vol. 73, pp. 101-105, 1871.

3. Bazin, H., "Experiments on Wave Propagation in Torrential Flow and Their Confirmation of the Boussinesq Equations for Gradually Varied Flow." Comptes Rendus des Seances de l'Academie des Sciences, Vol. 100, pp. 1492-1494, June 15, 1885.

4. Chow, V. T., "Rapidly Varied Unsteady Flow." Open Channel Hydraulics, Chapter 19, McGraw-Hill, 1959.

5. Favre, H., "Theoretical and Experimental Study of Translatory Waves in Open Channels," Dunod, Paris, 1935.

6. Gentilini, B., "L'Azione Di Uno Sfioratore Laterale Sull 'onda Positiva Ascendente in Un Canale," Memorie e Studi Dell'Istituto Di Idraulica e Costruzioni Idrauliche Del Politecnico Di Milano, Centro Lombardo Di Ricerche Idrauliche Del Consiglio Nazionale Delle Ricerche, No. 78, 1950.

7. Ippen, A. T. and Harleman, D.R.F., "Verification of Theory for Oblique Standing Waves." Proceedings, ASCE, Vol. 80, No. 526, October, 1954.

8. Jones, L. E., "Some Observations on the Undular Jump." Proceedings, ASCE (Journal of the Hydraulics Division), Vol. 90, No. HY3, May, 1964.

9. Keulegan, G. H. and Patterson, G. W., "Mathematical Theory of Irrotational Translation Waves." RP 1272, Journal of Research of the National Bureau of Standards, Vol. 24, January, 1940.

10. Keulegan, G. H., "Gradual Damping of Solitary Waves" Journal of Research of the National Bureau of Standards, Vol. 40, 1948.

11. McCowan, J., "On the Solitary Wave." The London, Edinburgh, and Dublin Philosophical Magazine and Journal of Science, Vol. 32 (5), 1891.

12. Mosonyi, E., Water Power Development, Vol. 1, 2nd English Edition, Publishing House of the Hungarian Academy of Sciences, Budapest, 1963.

13. Rayleigh, Lord, "On Waves." The London, Edinburgh, and Dublin Philosophical Magazine and Journal of Science, Ser. 5, Vol. 1, pp. 257-279, April, 1876.

14. Sandover, J.A., and Zienkiewicz, O.C., "Experiments on Surge Waves." Water Power, November, 1957.

15. Scott Russell, J., "Report on Waves." Report of the British Association for the Advancement of Science, 1844.

16. Stokes, G.G., "On Waves." Cambridge and Dublin Mathematical Journal, Cambridge, England, Vol. 8, 1847.

17. Thirriot, C., and Bednarczyk, S., "Ondulations Secondaires en Front D'Intumescences et Ondes Solitaires." La Houille Blanche, No. 8, 1964.

Table 1

COMPUTER DERIVED THEORETICAL PARAMETERS

| y_1	Fo	Equation (11)			Equation (12)		
		Vw	YAVE	YPK	Vw	YAVE	YPK
0.333	0.057	2.79	0.043	0.098	2.78	0.043	0.093
	0.115	2.73	0.088	0.201	2.73	0.088	0.195
	0.172	2.68	0.132	0.310	2.68	0.133	0.303
	0.230	2.64	0.178	0.429	2.63	0.179	0.419
	0.288	2.59	0.224	0.557	2.58	0.225	0.543
0.500	0.060	3.29	0.042	0.101	3.29	0.042	0.096
	0.119	3.23	0.085	0.205	3.22	0.085	0.199
	0.179	3.16	0.128	0.318	3.15	0.128	0.309
	0.239	3.10	0.172	0.439	3.09	0.173	0.427
	0.298	3.05	0.216	0.567	3.03	0.217	0.551
0.667	0.061	3.71	0.041	0.102	3.70	0.041	0.097
	0.122	3.63	0.083	0.207	3.62	0.083	0.201
	0.183	3.56	0.125	0.320	3.54	0.125	0.311
	0.245	3.49	0.168	0.442	3.47	0.168	0.428
	0.306	3.42	0.211	0.571	3.39	0.212	0.553

y_1 is in feet.
Vw is in feet per second.
Fo, YAVE, and YPK are dimensionless.

Table 2

EXPERIMENTAL DATA

y_1	Fo	Vw	Probe 1			Probe 3			Probe 5		
			YAVE	YPK	L	YAVE	YPK	L	YAVE	YPK	L
0.333	0.057	2.78	0.042	0.051	11.1	0.036	0.039	16.7	0.042	0.048	16.7
	0.115	2.84	0.072	0.072	10.0	0.078	0.087	14.2	0.081	0.096	17.0
	0.172	2.68	0.132	0.141	10.7	0.132	0.147	13.4	0.138	0.159	17.5
	0.230	2.73	0.180	0.183	8.2	0.177	0.196	13.6	0.168	0.174	15.0
	0.288	2.59	0.234	0.228	7.8	0.192	0.198	7.8	0.168	0.177	13.0
0.500	0.060	3.42	0.036	0.036	12.0	0.040	0.046	23.9	0.040	0.046	29.0
	0.119	3.41	0.080	0.084	11.9	0.082	0.096	20.5	0.076	0.090	20.5
	0.179	3.28	0.124	0.128	13.0	0.132	0.152	21.2	0.116	0.136	22.8
	0.239	3.20	0.156	0.166	12.8	0.152	0.172	20.8	0.144	0.160	19.2
0.667	0.061	3.94	0.039	0.039	15.8	0.033	0.037	25.6	0.042	0.045	31.5
	0.122	3.66	0.075	0.079	12.8	0.070	0.081	25.6	0.073	0.068	29.3
	0.183	3.57	0.117	0.121	12.9	0.120	0.139	23.2	0.108	0.125	33.9

y_1	Fo	Vw	Probe 2			Probe 4			Probe 6		
			YAVE	YPK	L	YAVE	YPK	L	YAVE	YPK	L
0.333	0.057	2.78	0.036	0.035	--	0.039	0.046	16.7	0.045	0.048	16.7
	0.115	2.84	0.072	0.072	8.5	0.084	0.096	15.6	0.084	0.105	18.5
	0.172	2.68	0.138	0.135	9.4	0.144	0.174	13.4	0.132	0.165	16.1
	0.230	2.73	0.162	0.192	3.5	0.174	0.216	13.6	0.168	0.198	13.7
	0.299	2.59	0.204	0.228	5.2	0.195	0.231	5.2	--	--	--
0.500	0.060	3.42	0.040	0.040	13.0	0.042	0.046	23.9	0.046	0.044	24.0
	0.119	3.41	0.080	0.084	11.9	0.080	0.096	20.5	--	--	--
	0.179	3.28	0.122	0.132	13.0	0.118	0.142	19.6	--	--	--
	0.239	3.20	0.148	0.160	12.0	0.152	0.172	20.8	--	--	--
0.667	0.061	3.94	0.045	0.045	13.8	0.037	0.045	25.6	0.039	0.039	31.5
	0.122	3.66	0.076	0.079	14.6	0.068	0.078	29.3	--	--	--
	0.183	3.57	0.120	0.127	16.1	0.114	0.130	23.2	--	--	--
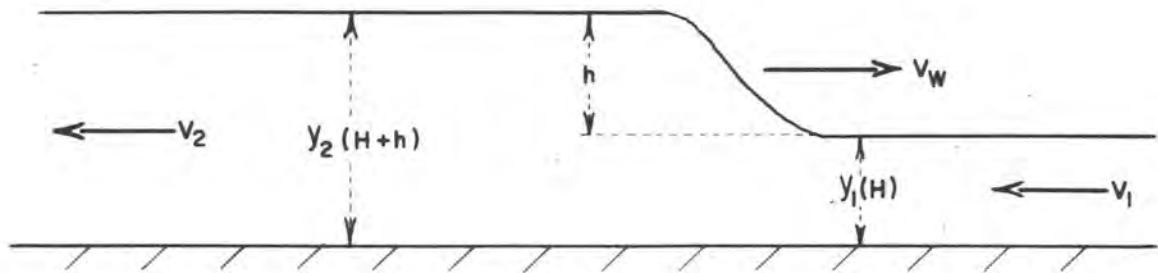
NOT TO SCALE
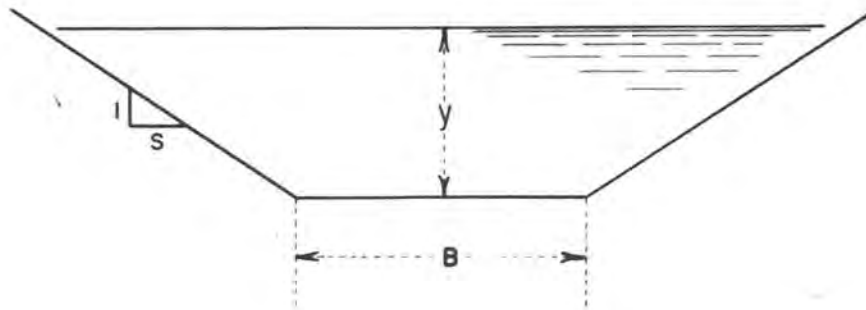
FIGURE 1

DEFINITION SKETCH FOR DERIVATIONS
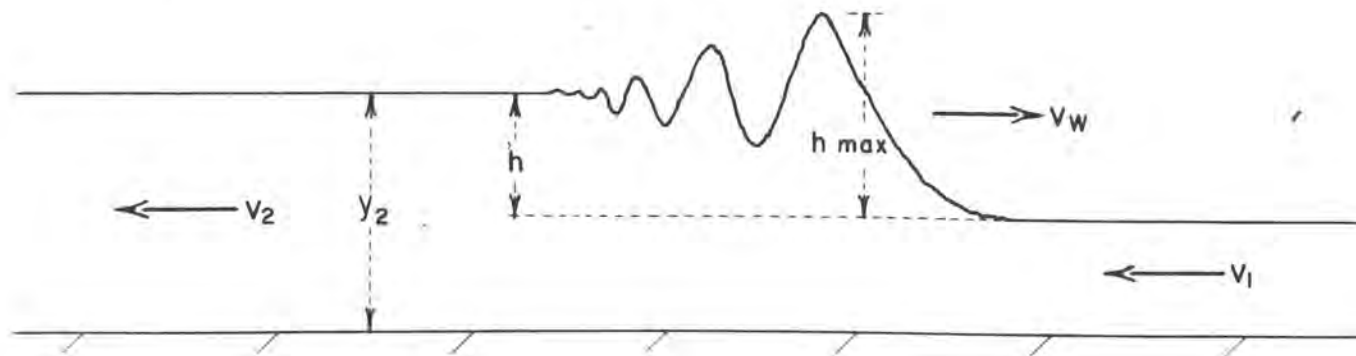
NOT TO SCALE—STEEPNESS OF PEAKS
IS EXAGGERATED.

FIGURE 2

DEFINITION SKETCH FOR UNDULAR FORM OF SURGE WAVE
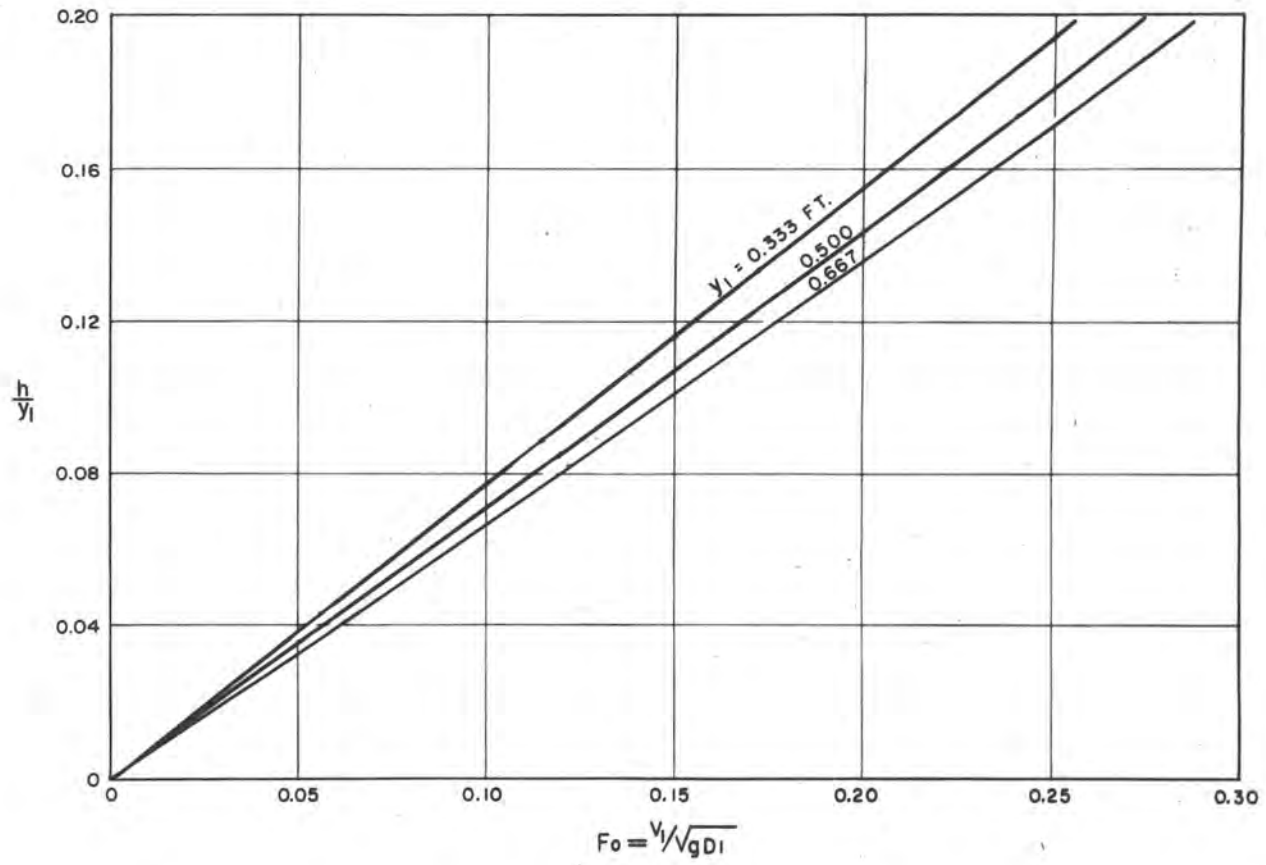
FIGURE 3

THEORETICAL RELATIONSHIPS--RATIO OF AVERAGE SURGE HEIGHT TO
INITIAL DEPTH VS FROUDE NUMBER OF INITIAL FLOW
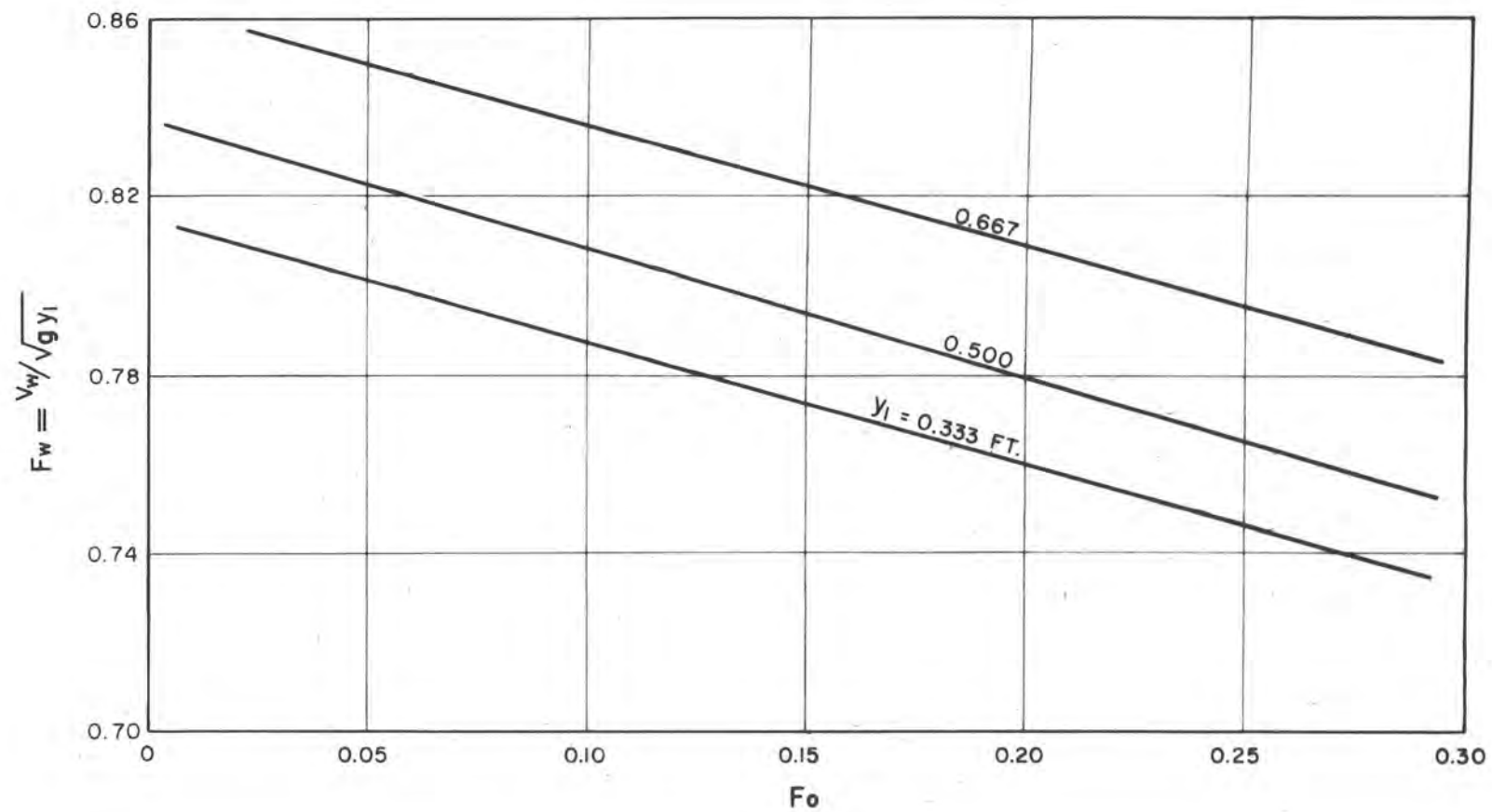
FIGURE 4

THEORETICAL RELATIONSHIPS--FROUDE NUMBER OF INITIAL FLOW VS

FROUDE NUMBER OF WAVE
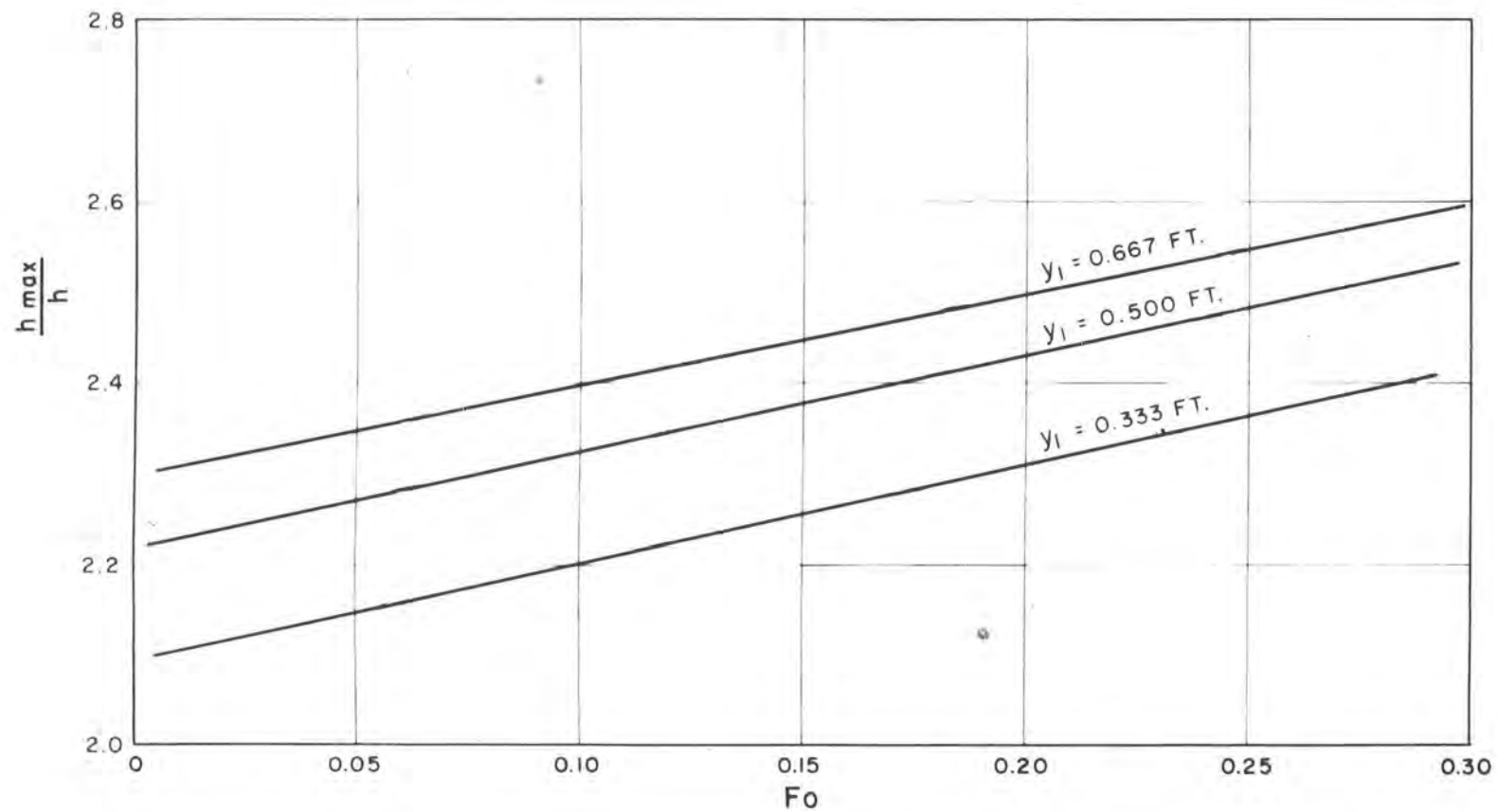
FIGURE 5

THEORETICAL RELATIONSHIPS--RATIO OF HEIGHT OF FIRST

OSCILLATION PEAK TO AVERAGE SURGE HEIGHT VS FROUDE NUMBER

OF INITIAL FLOW

SLIDE GATE

A →

HEADBOX

← 5'- 0" →

15'- 0"

15'- 0"

4'- 0"

2
+1

4
+3

6
+5

48'- 6"

+ I ETC. ARE PROBE
LOCATIONS

A →

FROM PUMP AND
ORIFICE METER--

PLAN (1" = 6')

PROBE 4

PROBE 3

1

1½

12"

6"

12"

SECTION A-A (1" = 1')
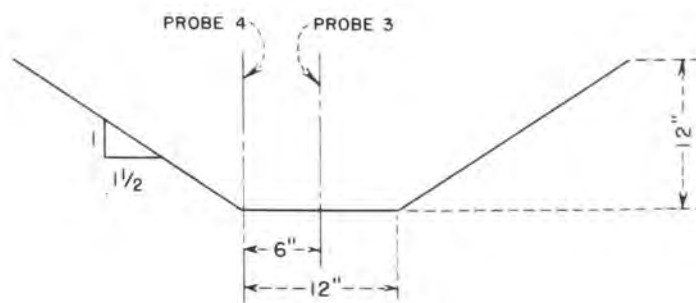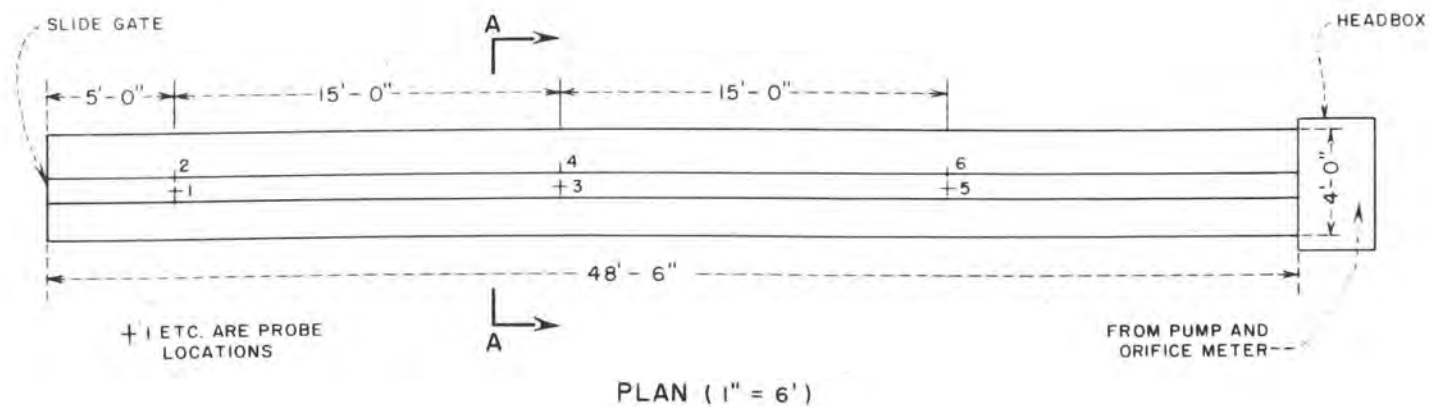
FIGURE 6

EXPERIMENTAL TEST CHANNEL AND PROBE LOCATIONS

FIGURE 7

PHOTOGRAPH OF TEST CHANNEL AND WAVE PROBES

R_1, R_2 = 200 to 250 ohms

C_1, C_2 = 0.1 microfarad, dual bathtub
               condenser preferred
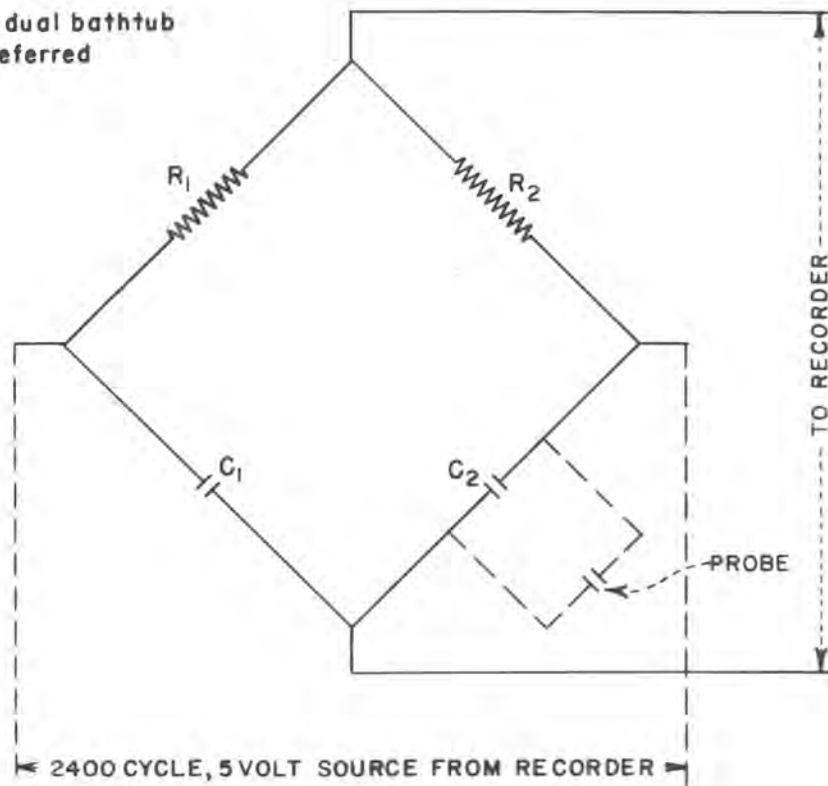
FIGURE 8

BRIDGE CIRCUIT FOR VARIABLE CAPACITANCE WAVE PROBE

FIGURE 9

PHOTOGRAPH OF TYPICAL REJECTION SURGE WAVE

PROBE 1

PROBE 2

0.02 foot

PROBE 3

1 second

PROBE 4

PROBE 5

PROBE 6
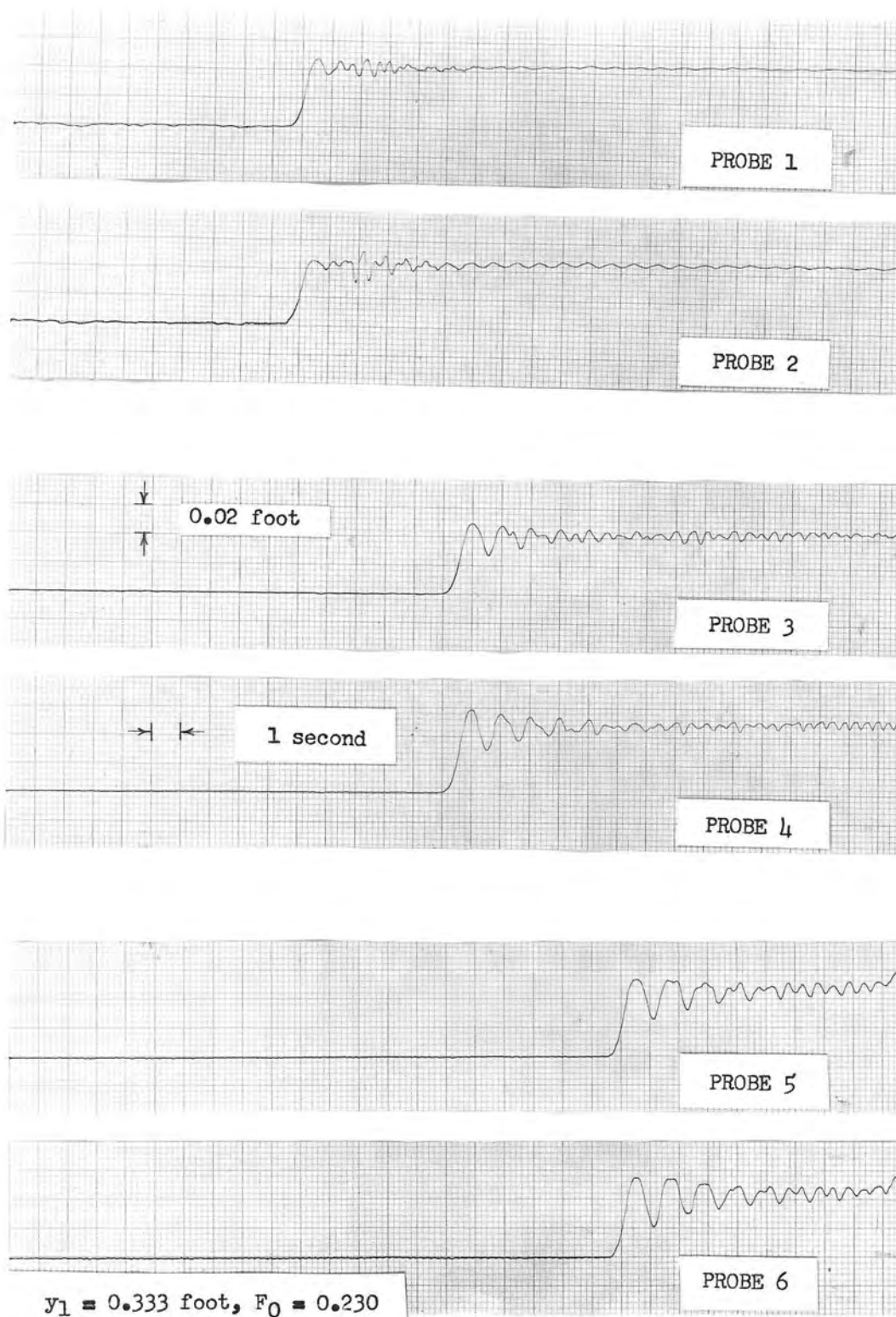
$y_1 = 0.333$ foot, $F_0 = 0.230$

FIGURE 10

RECORDING OF TYPICAL REJECTION SURGE WAVE
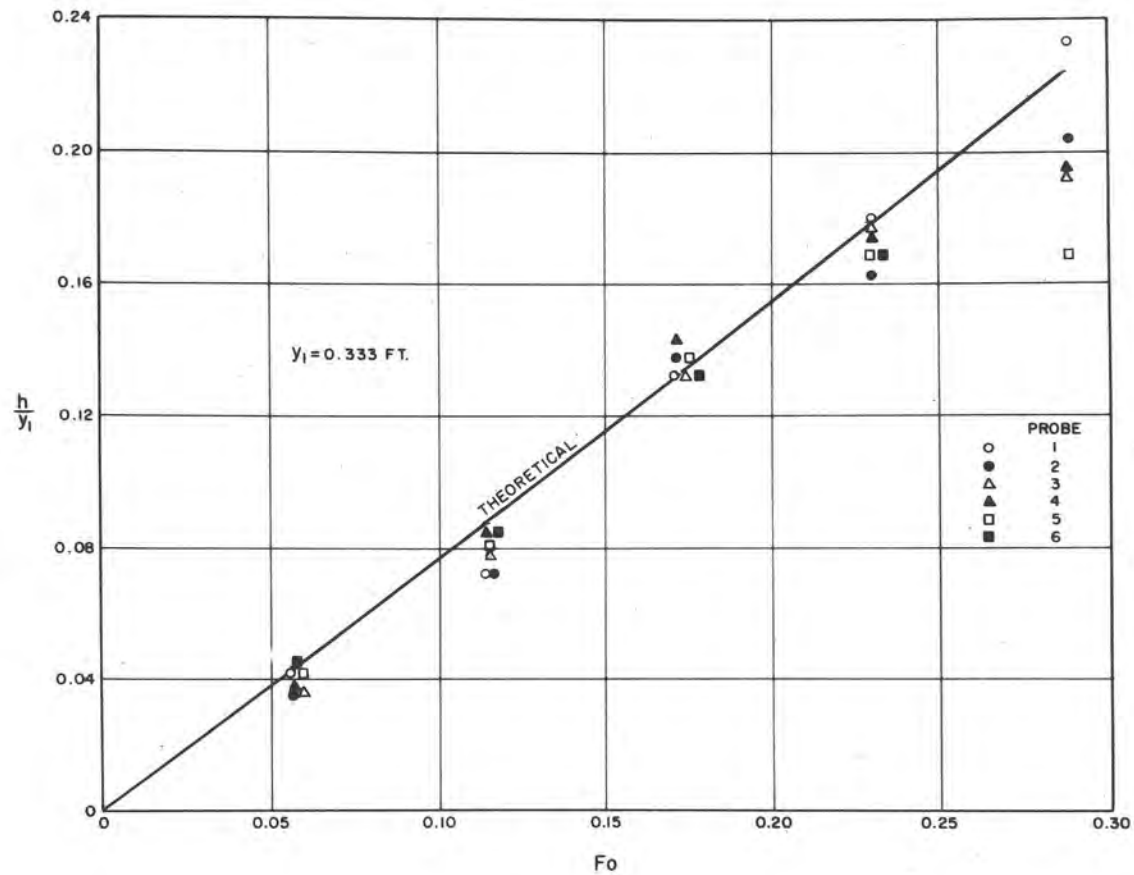
FIGURE 11

EXPERIMENTAL RELATIONSHIPS AND COMPARISON WITH THEORY--
RATIO OF AVERAGE SURGE HEIGHT TO INITIAL DEPTH VS FROUDE
NUMBER OF INITIAL FLOW, $Y_1 = 0.333$ FOOT
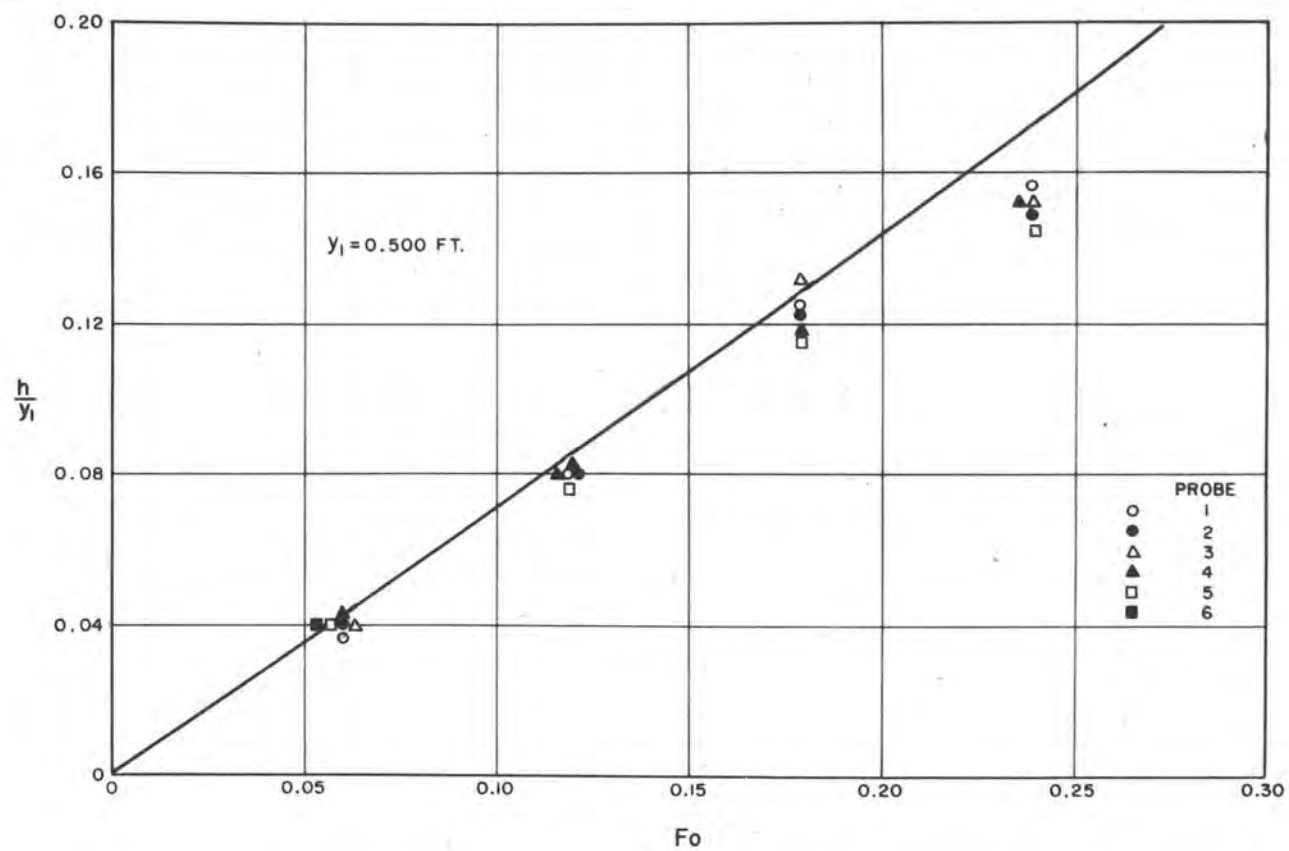
FIGURE 12

EXPERIMENTAL RELATIONSHIPS AND COMPARISON WITH THEORY--
RATIO OF AVERAGE SURGE HEIGHT TO INITIAL DEPTH VS FROUDE
NUMBER OF INITIAL FLOW, $Y_1 = 0.500$ FOOT
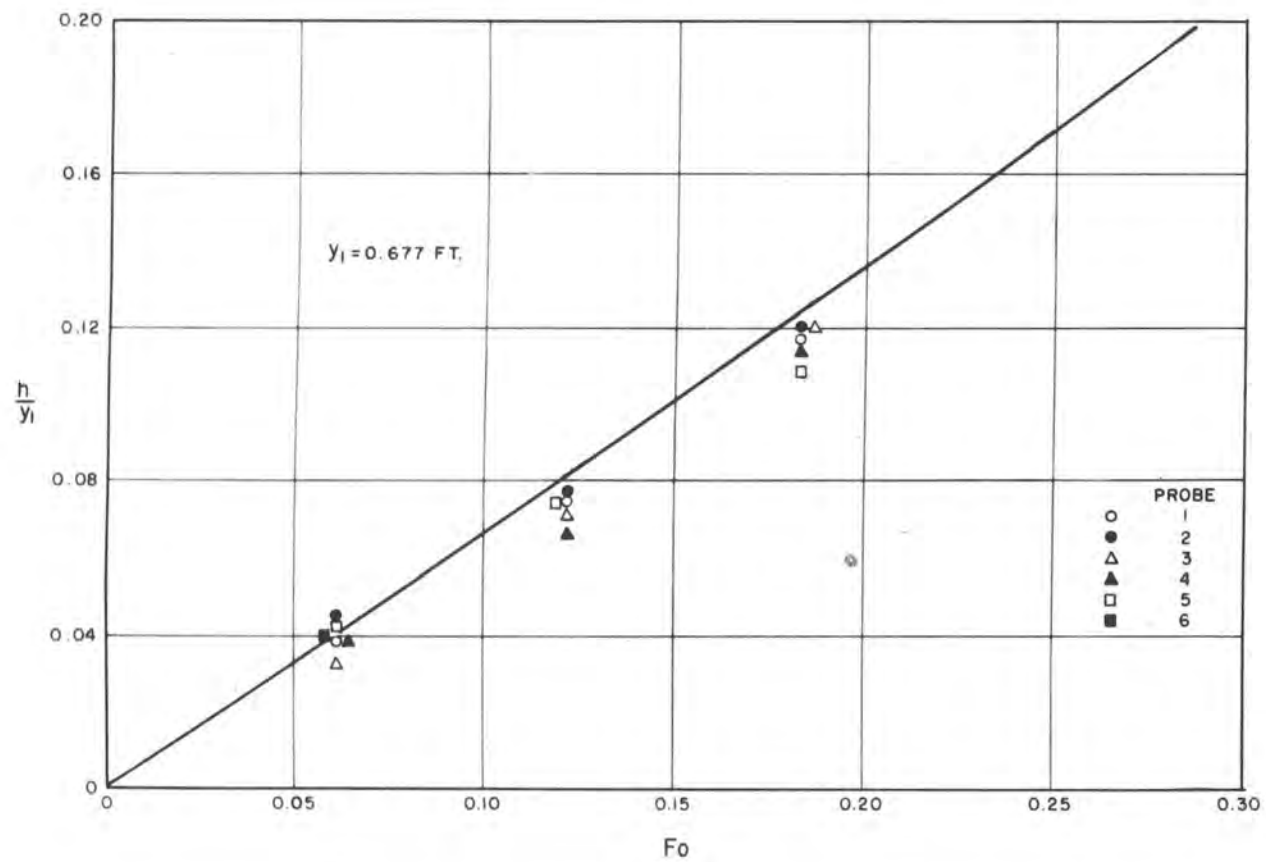
FIGURE 15

EXPERIMENTAL RELATIONSHIPS AND COMPARISON WITH THEORY--
RATIO OF AVERAGE SURGE HEIGHT TO INITIAL DEPTH VS FROUDE
NUMBER OF INITIAL FLOW, $Y_1 = 0.667$ FOOT
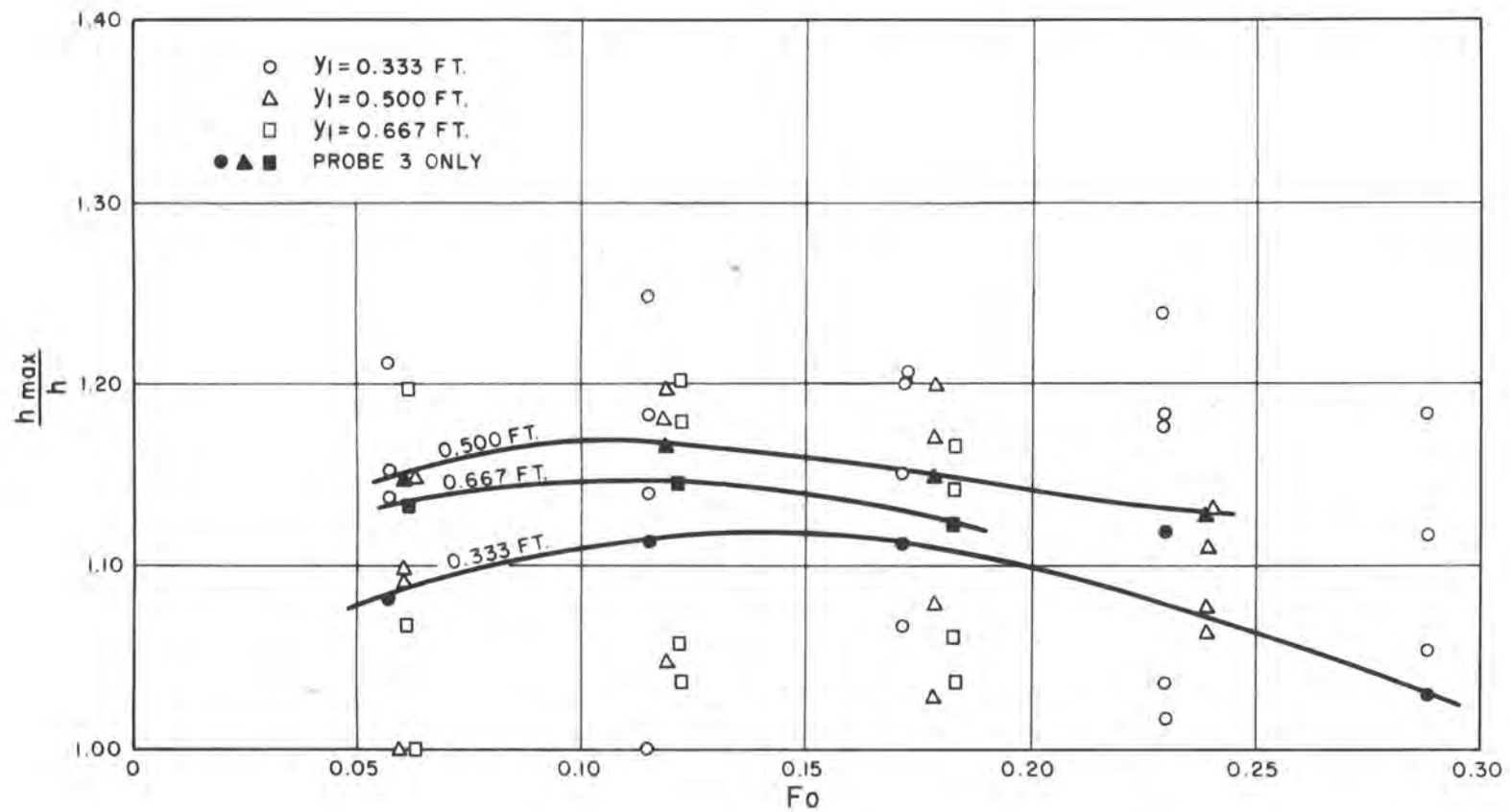
FIGURE 14

EXPERIMENTAL RELATIONSHIPS—RATIO OF HEIGHT OF FIRST

OSCILLATION PEAK TO AVERAGE SURGE HEIGHT VS FROUDE NUMBER OF INITIAL FLOW
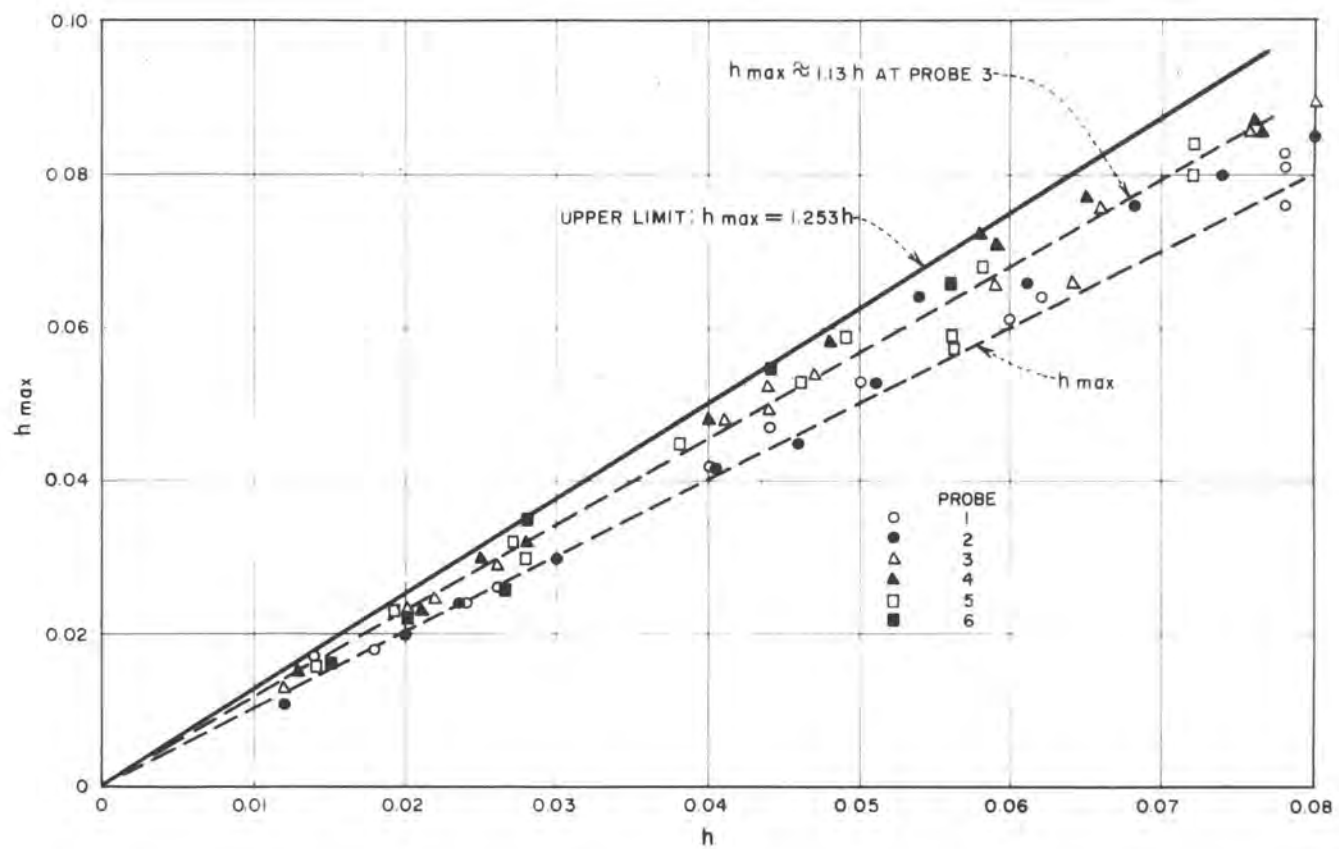
FIGURE 15

EXPERIMENTAL RELATIONSHIPS--AVERAGE SURGE HEIGHT VS

HEIGHT OF FIRST OSCILLATION PEAK
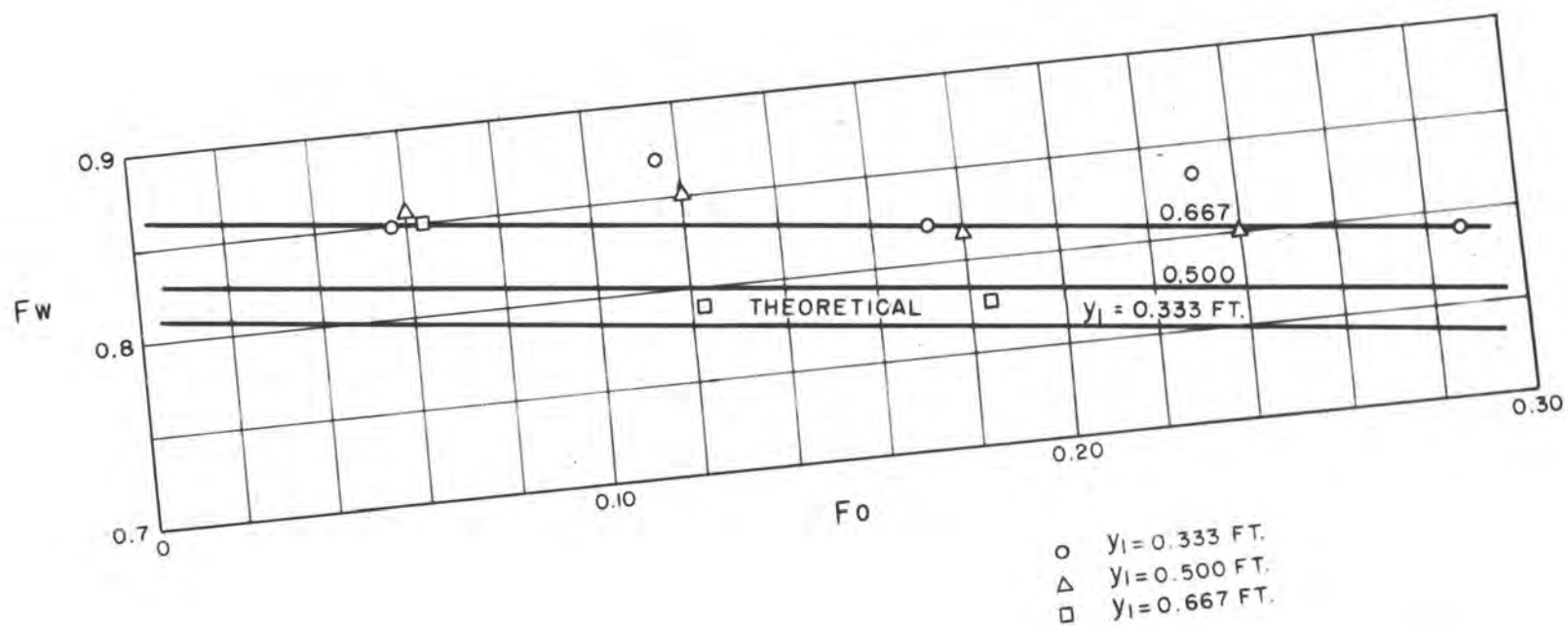
FIGURE 16

EXPERIMENTAL RELATIONSHIPS AND COMPARISON WITH THEORY--
FROUDE NUMBER OF INITIAL FLOW VS FROUDE NUMBER OF WAVE
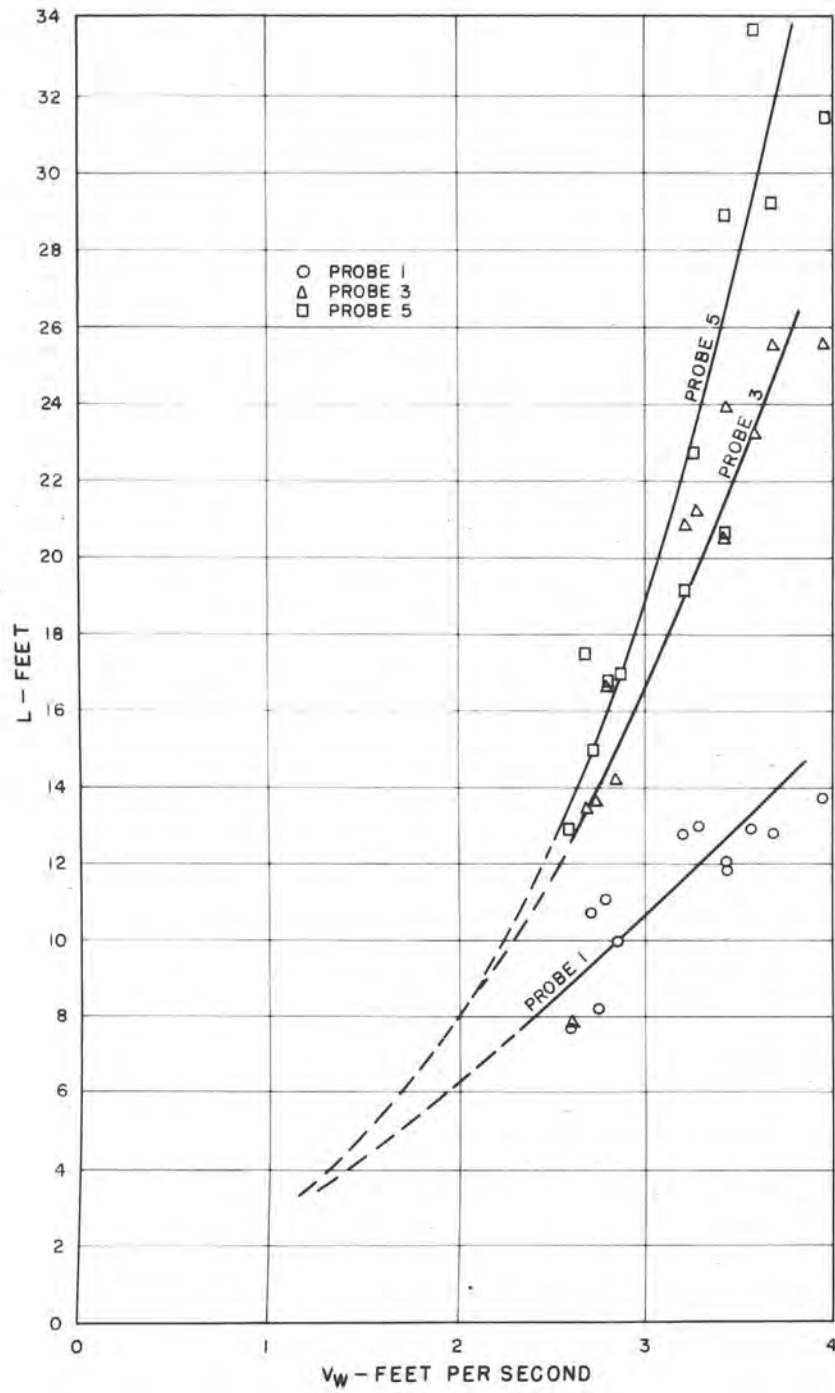
FIGURE 17

EXPERIMENTAL RELATIONSHIPS--WAVE VELOCITY VS FIRST

WAVE LENGTH

APPENDIX

DEFINITION OF TERMS* USED IN COMPUTER PROGRAM

Symbol	Units	Description
DELTA	Ft	Size of iteration steps
FF	Ft/sec	Indicator of accuracy of approximate solution
I	None	Loop counter
J	None	Loop counter
N	None	Number of iterations
PEAK	Ft	Maximum surge height (hmax)
QREJ	Ft^3/sec	Rejected discharge
RATIO	Dimensionless	hmax/h
SURGE	Ft	Average surge height (h)
YAVE	Dimensionless	h/y_1
YPK	Dimensionless	$hmax/y_1$
Y2MIN	Ft	Minimum value of y_2
Y2MAX	Ft	Maximum value of y_2
YBAR1	Ft	$\overline{y}_1$
YBAR2	Ft	$\overline{y}_2$

*Terms which are identical to those defined in the main body of the text are not repeated.

```
          C     HEIGHT OF REJECTION SURGE IN A TRAPEZOIDAL CHANNEL
0001         11 FORMAT (6F8.0,I4)                                                      4
0002         13 FORMAT (1X,6F10.3)                                                     5
0003         14 FORMAT (1H0,30H        INITIAL   BOTTOM    SIDE)                       7
0004        150FORMAT (60H         DEPTH    WIDTH     SLOPES     Q         QREJ         8
            1   F)                                                                    8A
0005        160FORMAT (1H0,69H          YAVE      YPK      RATIO      VW        C      9
            1       V1      FF)                                                       9A
0006         23 FORMAT (1X,6F10.3,F10.6)                                             10
0007         20 READ (5,11) Y,B,S,Q,QREJ,DELTA,N                                     11
0010            REJ=QREJ                                                             11A
0011            WRITE (6,14)                                                         12
0012            WRITE (6,15)                                                         13
0013            DO 600 J=1,4                                                         16
0014            Y1=Y                                                                 18
0015            Y2MIN=Y1                                                             19
0016            Y2MAX=Y1+DELTA                                                       20
0017            DO 100 I=1,N                                                         21
0020            Y2=(Y2MIN+Y2MAX)/2.0                                                 22
0021            YBAR1=Y1-Y1*(3.0*B+4.0*S*Y1)/(3.0*(2.0*B+2.0*S*Y1))                  23
0022            YBAR2=Y2-Y2*(3.0*B+4.0*S*Y2)/(3.0*(2.0*B+2.0*S*Y2))                  24
0023            A1=Y1*(B+S*Y1)                                                       25
0024            D1=A1/(B+2.0*S*Y1)                                                   50
0025            A2=Y2*(B+S*Y2)                                                       26
0026            V1=Q/A1                                                              27
0027            V2=(Q-QREJ)/A2                                                       27A
0030            OFF=SQRT((A2*YBAR2-A1*YBAR1)/(A1*(1.0-A1/A2)))-0.176*V1-0.176*(QREJ   28
            1/(A2-A1))                                                              29
0031            IF (FF .LT. 0.0) Y2MIN=Y2                                            30
0032            IF (FF .GT. 0.0) Y2MAX=Y2                                            31
0033            IF (FF .EQ. 0.0)GO TO 600                                            32
0034            IF (ABS(FF) .LE. 0.00001) GO TO 600                                  32A
0035        100 CONTINUE                                                             33
0036        600 SURGE=Y2-Y1                                                          48
0037            F=V1/SQRT(32.174*D1)                                                 51
0040            VW=REJ/(A2-A1)                                                       54
0041            C=VW+V1                                                              55
          C     CALCULATION OF OSCILLATION PEAKS                                     58
0042            DPEAK=C*C/32.174                                                     59
0043            IF (S .EQ. 0.0) PEAK=DPEAK                                           59AA
0044            IF (S .EQ. 0.0) GO TO 800                                            59BB
0045            OPEAK=-((B-2.0*S*DPEAK)/(2.0*S))+SQRT(ABS((B-2.0*S*DPEAK)/(2.0*S))    59CC
            1**2+(B*DPEAK/S))                                                       59DD
0046        800 YAVE=(Y2-Y1)/Y1                                                      59A
0047            YPK=(PEAK-Y1)/Y1                                                     60
0050            RATIO=YPK/YAVE                                                       61
0051            WRITE (6,13) Y,B,S,Q,QREJ,F                                          64
0052            WRITE (6,16)                                                         14A
0053            WRITE (6,23) YAVE,YPK,RATIO,VW,C,V1,FF                               67
0054            GO TO 20                                                             72
0055            END

            Alternate for IFN 0030:

            OFF=SQRT(32.174*D1)*(1.0+((.0-2.0*S/3.0*D1/(B+2.0*S*Y1))*0.75*(Y2-Y    28
            1)/D1)-V1-(QREJ/(A2-A1))                                               29
```

LISTING OF PROGRAM SOURCE STATEMENTS

LABORATORY PUNCH CARD DATA

BUREAU OF RECLAMATION

USE	PROBLEM	Sample Input Data Sheet	JOB NO.		
COLORED CARDS	DETAIL	for Theoretical Computation	# Sample		
	FEATURE	of Rejection Surge Heights	RETURN TO		
	PROJECT		ROOM	BLDG.	PHONE

Y	B	S	Q	QREJ	DELTA	N				
0.333	1.0	1.5	0.081	0.081	1.0	50				
0.333	1.0	1.5	0.163	0.163	1.0	50				
0.333	1.0	1.5	0.244	0.244	1.0	50				
0.333	1.0	1.5	0.326	0.326	1.0	50				
0.333	1.0	1.5	0.408	0.408	1.0	50				

REMARKS

BY	DATE	CHECKED	SHEET 1 OF 1

GPO 833969

INITIAL DEPTH	BOTTOM WIDTH	SIDE SLOPES	Q	QREJ	F	
.333	1.000	1.500	.081	.081	.057	

YAVE	YPK	RATIO	VW	C	V1	FF
.043	.098	2.269	2.785	2.947	.162	.000003

INITIAL DEPTH	BOTTOM WIDTH	SIDE SLOPES	Q	QREJ	F	
.333	1.000	1.500	.163	.163	.115	

YAVE	YPK	RATIO	VW	C	V1	FF
.088	.201	2.291	2.733	3.059	.326	.000006

INITIAL DEPTH	BOTTOM WIDTH	SIDE SLOPES	Q	QREJ	F	
.333	1.000	1.500	.244	.244	.172	

YAVE	YPK	RATIO	VW	C	V1	FF
.132	.310	2.347	2.683	3.172	.489	-.000008

INITIAL DEPTH	BOTTOM WIDTH	SIDE SLOPES	Q	QREJ	F	
.333	1.000	1.500	.326	.326	.230	

YAVE	YPK	RATIO	VW	C	V1	FF
.178	.429	2.412	2.635	3.288	.653	.000002

SAMPLE OUTPUT LISTING

4